AIMS Energy, 9(4): 830–841.
DOI: 10.3934/energy.2021038
Received: 31 May 2021
Accepted: 21 June 2021
Published: 28 June 2021

http://www.aimspress.com/journal/energy

Research article

Effect of Ag NPs on the radiant absorption of photocatalyst film

Jiayu Li* and Jiewen Guo

MIIT Key Laboratory of Thermal Control of Electronic Equipment, School of Energy and Power Engineering, Nanjing University of Science and Technology, Nanjing 210094, China

* **Correspondence:** Email: lijiayu@mail.njust.edu.cn; Tel: +15051807486.

Supplementary Information

S1. Photocatalytic activities of prepared Ag/Al_2O_3-TiO_2 films

1.1. Ag/Al_2O_3-TiO_2 film preparation

Composite films were prepared layer-by-layer using a high-vacuum magnetron sputtering system (JGP-450A). The substrate was a borosilicate glass wafer with a diameter of 20 mm and a thickness of 2 mm. Before deposition, the substrates were preprocessed through sequential ultrasonic cleaning in acetone and alcohol baths and then dried in N_2. Ag, Al_2O_3 and TiO_2 targets with the same diameter of 60 mm and the same purity of 99.99% were utilized. The working gas was argon (Ar) with flow rate of 60 mL/min. The Ag/Al_2O_3 film prepared through cosputtering was deposited on the substrate. Radio-Frequency (RF) magnetron sputtering with a power of 110 W was used for Al_2O_3 targets, and the Direct-Current (DC) magnetron sputtering with power of 8 W was used for Ag target. The fraction of Ag in the Ag/Al_2O_3 film was controlled by the sputtering power, whereas the diameter and distribution of Ag NPs were random. The sputtering progress was sketched in Figure S1. The deposition time of Al_2O_3 target was longer than that of the Ag target, given that Ag NPs were prepared to be immersed in Al_2O_3. The TiO_2 film was deposited on the Ag/Al_2O_3 film through RF magnetron sputtering with power of 85 W. The thickness of the TiO_2 film and the distance between Ag and TiO_2 was manually regulated by controlling the deposition time of each target. The details of deposition conditions were summarized in Table S1.

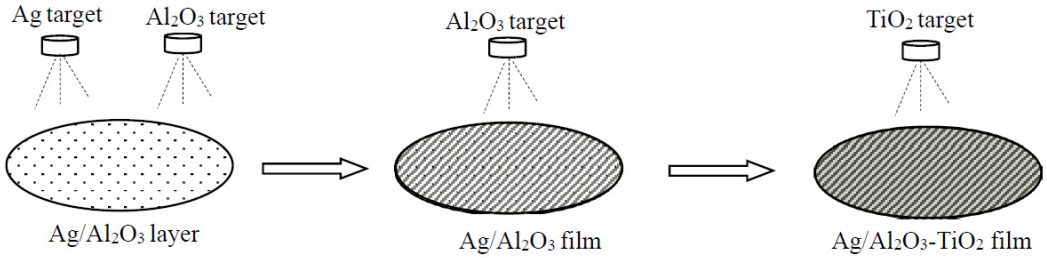

Figure S1. The flow chart of sputtering progress.

Table S1. Deposition conditions of composite films.

Sample ID	TiO_2 layer		Al_2O_3 layer			Ag/Al_2O_3 layer	
	Target	Deposition time/min	Target	Deposition time/min	Thickness/nm	Target	Deposition time/min
I-2 nm	TiO_2	90	Al_2O_3	1.32	2	Al_2O_3 Ag	30
II-5 nm	TiO_2	90	Al_2O_3	3.32	5	Al_2O_3 Ag	30
III-10 nm	TiO_2	90	Al_2O_3	6.65	10	Al_2O_3 Ag	30
IV-15 nm	TiO_2	90	Al_2O_3	10	15	Al_2O_3 Ag	30
N-Al_2O_3-TiO_2	TiO_2	90	Al_2O_3	66.5	100	/	/
T-Ag/Al_2O_3	/	/	Al_2O_3	3.32	5	Al_2O_3 Ag	30

The deposition conditions listed in Table S1 indicated that the sputtering progress for Ag/Al_2O_3 layer was the same for each sample (Sample I-2 nm to IV-15 nm, and T-Ag/Al_2O_3), so their nanostructures would be similar, the nanostructure of Sample T-Ag/Al_2O_3 was investigated by TEM. Two images were randomly picked, which was shown in Figure S2(a) and (b). As the image of Ag was significantly darker than that of Al_2O_3, it was easy to find that the distribution and morphology of Ag particles were random. Ag NPs were prone to aggregate in the composite film, which was especially obvious in Figure S2(b). The TEM images also indicated that the sizes of most Ag NPs immersed in Al_2O_3 host were less than 100 nm. The dispersion of Ag particles was limited by the RF magnetron sputtering method. The power for Ag target should be much lower than that for the Al_2O_3 target to enhance Ag dispersion in Al_2O_3 host. In actual coating, the sputtering power on the Ag target should be above a certain value, and the Al_2O_3 target would crack when the sputtering power for the Al_2O_3 target was excessively high. The distance between Ag NPs and TiO_2 layer could be regulated by controlling the deposition time of Al_2O_3 target, while the morphology, size and distribution of Ag NPs in the composite films could not be regulated precisely.

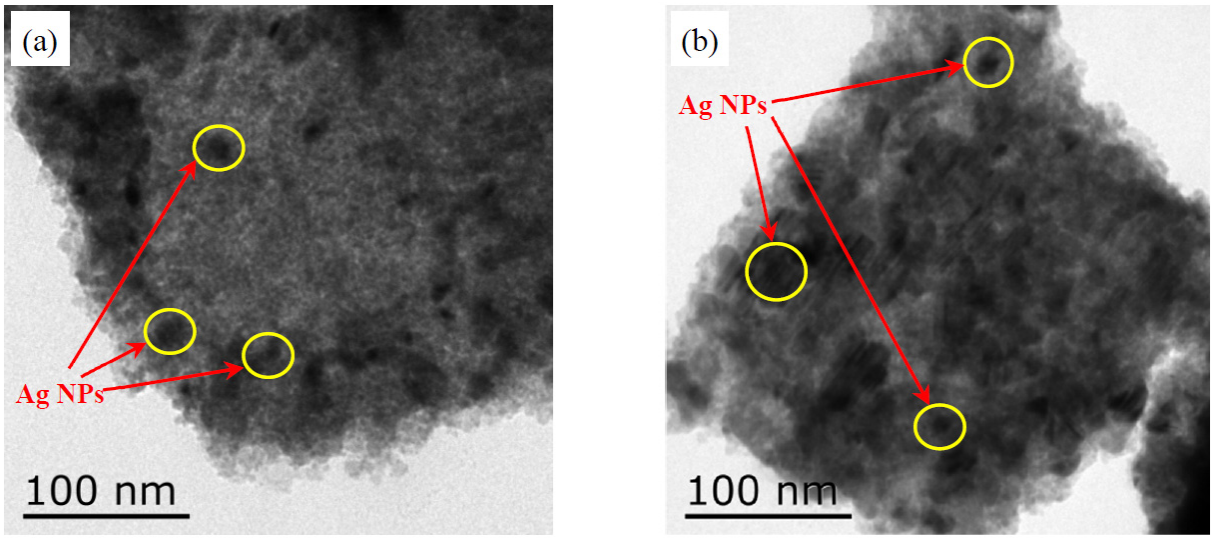

Figure S2. TEM images of the Ag/Al_2O_3 composite film nanostructure.

1.2. Characterization of the Photocatalytic Activity of Ag/Al_2O_3-TiO_2 film

The photocatalytic activities of Ag/Al_2O_3-TiO_2 films with different Ag-TiO_2 spacings were compared based on their degradation of aqueous methylene blue (MB) under the irradiation of HPMV without filter. The spectrum and illumination intensity of the HPMV were shown in Figure S3. Each composite film was immersed in 40 mL MB solution with the concentration of 5 mg/L. The incident source (HPMV) was just above the sample with the distance of 250 mm between them. The degradation fraction of aqueous methylene blue was analyzed via its absorption peak measured with UV-VIS spectrophotometer, which was expressed as follows:

$$\text{Degradation fraction (\%)} = \frac{A_0 - A}{A_0} \times 100\% \quad \text{(S1)}$$

where A_0 was the absorbance of methylene blue solution in adsorption equilibrium at the wavelength of 666 nm where the solution absorption peak was located. A was the absorbance of the methylene blue solution at 666 nm after catalytic degradation. The degradation fractions for Ag/Al_2O_3-TiO_2 films listed in Table 1 were compared in Figure S4. "M.B." represented the degradation of methylene blue solution in the absence of a photocatalyst. The degradation time was 50 min. The degradation rate of the methylene blue solution was increased due to the presence of Ag NPs. As shown in Figure S4, the degradation rate of sample IV-15 nm, which have 15 nm Ag-TiO_2 spacing filled with Al_2O_3 is the lowest. Meanwhile, the sample I-2 nm, which have 2 nm Ag-TiO_2 spacing filled with Al_2O_3 have the best photocatalytic degradation rate of the methylene blue solution. The catalytic activity of the composite film with 2 nm Ag-TiO_2 distance was close to that of the composite film with 5 nm Ag-TiO_2 distance (II-5 nm). Thus, the thin Ag-TiO_2 spacing of 2 nm or 5 nm was beneficial to the photocatalytic activity.

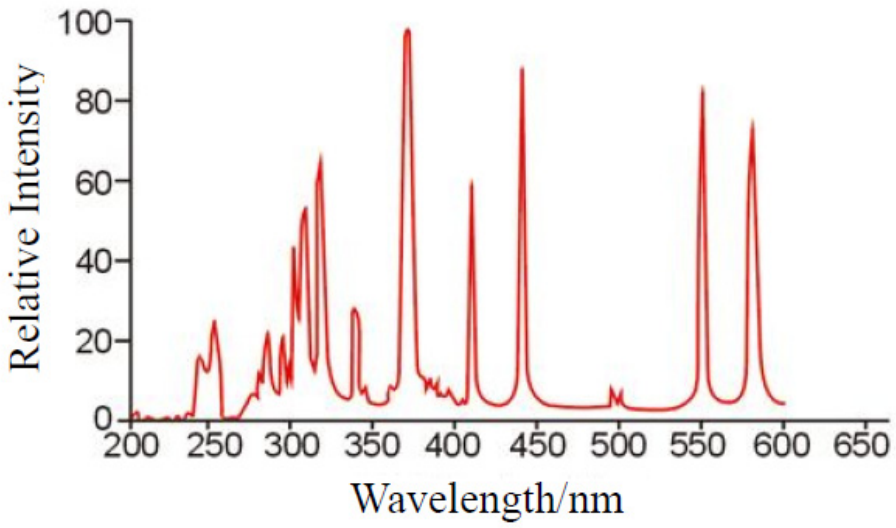

Figure S3. The spectrum and relative intensity of the HPMV.

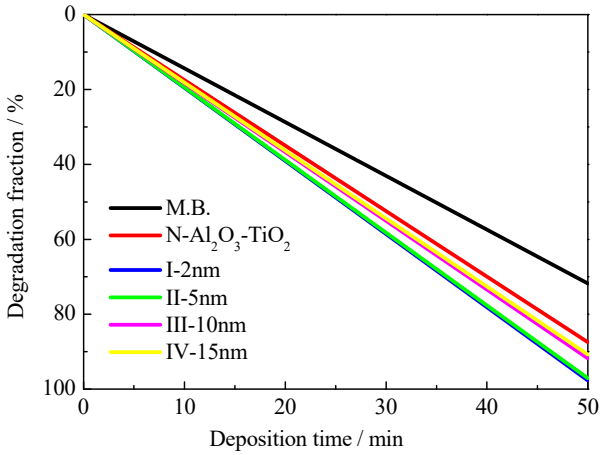

Figure S4. Degradation fractions of methylene blue for Ag/Al_2O_3-TiO_2 films with different Ag-TiO_2 spacings under the irradiation of HPMV.

Photocatalytic reactions are mainly driven by charge carriers which are generated by incident irradiation. In the irradiated composite film of Ag/Al_2O_3-TiO_2, the enhanced localized radiant absorption caused by Ag NPs can significantly generate electrons and holes. The efficient utilization of charge carriers should be considered for photocatalytic reactions, which include the improvements of charge carrier generation, separation and migration. Only photogenerated charges that migrated to the surface of the as-prepared composite photocatalyst could promote the photoreaction. Figure S4 shows that the activity of the composite photocatalyst is influenced by the distance between Ag and TiO_2. The composite film with 2 nm or 5 nm Ag-TiO_2 distance possessed high catalytic activity, this result was similar to the result in Ref. [S1]. Because the sample and experimental conditions were not exactly the same as those in Ref. [S1], the degradation fractions and time could not be compared quantitatively.

The morphology and distribution of Ag NPs were not tailored exactly during the process of film

preparation. Thus, the influence of Ag NPs morphology was not analyzed experimentally. Based on the mechanism of photocatalytic reactions, the spectrum and distribution of radiant absorption in the photocatalyst film are two important factors for the improvement of the photocatalytic reaction. A theoretical model was constructed to analyze the distributions of localized radiant absorption in the composite films with different Ag NP nanostructures in this work.

S2. The Theory for the Radiant absorption model of composite film

The radiant absorption model for Ag/Al_2O_3-TiO_2 composite film was established based on electromagnetic theory. As Maxwell's equations are fundamental laws governing the behavior of a electromagnetic field in the medium [S2], the electromagnetic field in irradiated homogeneous isotropic medium could be described as follows:

$$\nabla \times \boldsymbol{E} = -\mu \frac{\partial \boldsymbol{H}}{\partial t} \tag{S2}$$

$$\nabla \times \boldsymbol{H} = \varepsilon \frac{\partial \boldsymbol{E}}{\partial t} + \sigma \boldsymbol{E} \tag{S3}$$

where $\boldsymbol{E}$ (V/m) is the electric field strength, $\boldsymbol{H}$ (A/m) is magnetic field strength, they are functions of position and time. μ is the permeability, ε is the permittivity, σ is conductivity, they are electromagnetic properties of the medium. The electromagnetic energy flow is governed by the time-averaged Poynting's power density vector $\boldsymbol{S}_{av}$:

$$\boldsymbol{S}_{av} = \frac{1}{2}\mathrm{Re}\{\boldsymbol{E} \times \boldsymbol{H}^*\} \tag{S4}$$

Then the rate of electromagnetic energy W_{abs} absorbed by the volume inclosed by surface A can be deduced. When I_i is the incident irradiance, the absorption cross section C_{abs} and absorption efficiency Q_{abs} of the particle can be expressed as follows [S3]:

$$C_{abs} = {W_{abs}}/{I_i} \tag{S5}$$

$$Q_{abs} = {C_{abs}}/{G} \tag{S6}$$

where G is the particle cross-sectional area projected onto a plane perpendicular to the incident beam.

From the theory above, the electromagnetic field ($\boldsymbol{E}$, $\boldsymbol{H}$) in irradiated composite film is the prerequisite for the properties of radiant absorption. The Finite Difference Time Domain (FDTD) method is the most direct method to obtain the electromagnetic field ($\boldsymbol{E}$, $\boldsymbol{H}$) in irradiated composite film by solving the finite-differenced Maxwell's Eqs (S2) and (S3).

This computational process was implemented by commercial FDTD package. The electromagnetic properties of Ag NPs, Al_2O_3 host medium and TiO_2 film were specified by assigning these parameters inside each computational domain. To test the accuracy of the simulation, the simulated results through FDTD method was compared with those from measurement and Mie theory. The parameters, such as mesh resolution, boundary conditions, were set based on the comparison.

References

S1. Awazu K, Fujimaki M, Rockstuhl C, et al. (2008) A plasmonic photocatalyst consisting of silver nanoparticles embedded in titanium dioxide. *J Am Chem Soc* 130: 1676–1680.
S2. Kong JA (1986) Electromagnetic Wave Theory, New York: Wiley, 9–15.
S3. Bohren CF, Huffman DR (1983) Absorption and scattering of light by small particles, New York: Wiley, 63–73.

AIMS Press